Available online at www.sciencedirect.com

ScienceDirect

Advances in Space Research 66 (2020) 505–519

ADVANCES IN SPACE RESEARCH (a COSPAR publication)

www.elsevier.com/locate/asr

Marine gravity anomaly mapping for the Gulf of Tonkin area (Vietnam) using Cryosat-2 and Saral/AltiKa satellite altimetry data

Van-Sang Nguyen [a], Van-Tuyen Pham [a], Lam Van Nguyen [a,b], Ole Baltazar Andersen [c], Rene Forsberg [c], Dieu Tien Bui [d,e,*]

[a] Department of Geodesy, Faculty of Geomatics and Land Administration, Hanoi University of Mining and Geology, No. 18 Pho Vien, Duc Thang, Bac Tu Liem, Hanoi 10000, Viet Nam

[b] Department of Ocean Operations and Civil Engineering, Faculty of Engineering, Norwegian University of Science and Technology (NTNU), Larsgårdsvegen 2, 6025 Ålesund, Norway

[c] DTU Space, Technical University of Denmark, 2800 Kgs. Lyngby, Denmark

[d] Institute of Research and Development, Duy Tan University, Da Nang 550000, Viet Nam

[e] Geographic Information Science Group, Department of Business and IT, University of South-Eastern Norway, N-3800, Bø i Telemark, Norway

Received 28 November 2019; received in revised form 29 April 2020; accepted 30 April 2020
Available online 12 May 2020

Abstract

Marine gravity anomalies are essential data for determining coastal geoid, investigating tectonics and crustal structures, and offshore explorations. The objective of this study is to present a methodology for estimating marine gravity anomalies from CryoSat-2 and Saral/AltiKa satellite altimeter data for the Gulf of Tonkin of Vietnam with a high-resolution $2' \times 2'$ grid. A total of 15,665 sea surface height (SSH) grid points, including derived from the Cryosat-2 (6842 grid points) and Saral/AltiKa (8823 grid points) satellite altimeter data were used. Then, the remove-restore technique and the crossover adjustment algorithm were used to remove the long-wavelength geoid height, the mean dynamic topography (h_{MDT}), and time-varying sea-surface topography (h_t). The residual geoid heights (ΔN) were used to determine the residual gravity anomalies (δg) using the Least-Squares Collocation method, whereas the Earth Geopotential Model was employed to restore the long-wavelength gravity anomalies (Δg_{EIGEN}). GPS/leveling and tidal gauge of 31 tidal stations were used for assessing and choosing the best Earth Geopotential Model and Mean Dynamic Topography models for the study area (EIGEN6C4 and DTU15MDT models). The accuracy of the final marine gravity anomaly result was assessed using 56,978 marine gravity points, which were distributed in the study area. The result showed that the standard deviation between the satellite-derived gravity anomalies and checked points is ± 3.36 mGal, indicating good accuracy. After improving with ship-measured gravity anomalies, the accuracy of satellite-derived marine gravity anomaly improves to ± 2.63 mGal. The results of this research are useful for geodetic and geophysical applications in the region.

Keywords: Satellite altimetry; Marine gravity anomalies; Least-squares collocation; Gulf of Tonkin; South China Sea, Vietnam

1. Introduction

Gravity anomaly plays a vital role in studying tectonics, sub-surface geological structure, and offshore explorations (Hackney and Featherstone, 2003). Besides, the gravity anomaly data can be used for defining the geoid model (Hackney and Featherstone, 2003), building global

* Corresponding author at: Institute of Research and Development, Duy Tan University, Da Nang 550000, Viet Nam.

E-mail addresses: nguyenvansang@humg.edu.vn (V.-S. Nguyen), lam.v.nguyen@ntnu.no (L. Van Nguyen), oa@space.dtu.dk (O.B. Andersen), rf@space.dtu.dk (R. Forsberg), buitiendieu@duytan.edu.vn, dieu.t.bui@usn.no (D. Tien Bui).

https://doi.org/10.1016/j.asr.2020.04.051
0273-1177/

high-resolution gravity models for climate studies (Andersen et al., 2010, Liu et al., 2016), and several geodetic and geophysical applications (Hwang et al., 2004). In the oceanography area, gravity anomaly has been considered as an essential data source for ocean exploration (Fairhead et al., 2001, Haxby et al., 1983, Ruiz Etcheverry et al., 2015), seafloor depth and topography studies (Sandwell et al., 2014, Zhang et al., 2003), planning shipboard surveys (Gaina et al., 1998), tectonic structure investigations (Haxby et al., 1983), and inertial navigation and petroleum explorations (Sandwell and Smith, 1997).

Gravity data can be obtained directly by ship measurements and indirectly from dedicated satellite missions and altimetry (Noréus et al., 1997, Subrahmanyam et al., 1999). The ship-based method is capable of acquiring both high-quality and high-resolution data. However, this is a time-consuming method, and therefore, this data is mainly used as reference data. In contrast, the satellite-based method provides data with high temporal resolution and several mGal level accuracies. Therefore, it is an important data source for determining the gravity on large scales. Literature review shows that altimetry satellites, for example, Geodetic Mission such as Geosat or ERS-1 (Marks, 1996, Sandwell, 1992, Sandwell and McAdoo, 1988, Zhang and Blais, 1995), Jason-1 (Zhang et al., 2017), provide useful data sources for gravity-anomaly assessments due to continuous improvement of precision and spatial resolution.

Consequently, data from multiple satellites such as ERS-1, GEOSAT, Cryosat-2, and AltiKa have successfully been used to improve the resolution and precision of marine gravity models (Hwang et al., 2002, Hwang and Parsons, 1996, Zhang et al., 2017). The Delay-Doppler altimeter accuracy on CryoSat-2 has higher range precision than ERS-1 and Geosat altimeters, and in theory, its range precision can be obtained at a 1-cm level for 1 Hz data (Andersen, 2013). In general, the range precision level depends on where the observations are taken, i.e., coast, shelf, open ocean, in which operational modes they were taken, and how the data was processed. Fenoglio-Marc et al. (2015) found 6–8 cm RMS (root mean square) accuracy in the German Bight bight area of the North Sea with CryoSat-2 altimeter data in SAR mode. Calafat et al. (2017) showed accuracies of around 7 cm with CryoSat-2 and Jason-2 altimeter data over the ocean. Idžanović et al. (2017) indicated 3–5 cm accuracy for the coastal region of Norway with CryoSat-2 data. In more recent research, Verron et al. (2018) found 3–4 cm at the Issykkul lake (Kyrgyzstan) with Saral/AltiKa data.

In recent works, Andersen et al. (2013) computed gravity anomalies with high accuracy of approximately 2.5–3.5 mGal for Northwest Atlantic and Arctic Ocean areas using the remove-restore method, the crossover adjustment algorithm, and the LSC and FFT method. According to Sandwell and Smith (2009b), the error on gravity anomalies can be reduced by 40% with the use of the retracted altimeter waveforms method, the EGM2008 global gravity model, and the biharmonic spline interpolation method.

Studies of marine gravity anomalies have been considered in Vietnam in recent years. The Hanmet International gravity formula (Trung et al., 2018) was used to compute gravitational anomalies over Tonkin gulf belonging to the South China Sea, where marine satellite-derived gravity data were combined with land-based gravity. After that, the Moho depth points were calculated by examining and refining the 3D inverse gravity solution Sandwell et al. (2014)

Nevertheless, no attempt has so far been carried out on estimating marine gravity anomalies with high resolution and accuracy. The main objective of this study is to present a methodology for estimating marine gravity anomalies for the Gulf of Tonkin (Vietnam). For this task, the Cryosat-2 and Saral/AltiKa satellite altimeter data were used. The remove-restore technique and the crossover adjustment algorithm were used to remove the long-wavelength geoid height (N_{EIGEN}), the mean dynamic topography (h_{MDT}), and time-varying sea-surface topography (h_t). Subsequently, the residual geoid heights (ΔN)were used to determine the residual gravity anomalies (δg) with the use of the LSC method, whereas the Earth Geopotential Model (EIGEN-6C4) was employed to restore the long-wavelength gravity anomalies (Δg_{EIGEN}). Gravity anomaly calculated from satellite altimetry data had been fitted with 2011 ship-borne gravity anomaly points. The accuracy of the final marine gravity anomaly result was assessed by using the 56,978 ship-measured gravity anomalies points in the study area.

2. Study area and data

2.1. Description of the study area

Gulf of Tonkin, covering an area about 127,000 km^2, is located between longitudes 105°40′E and 110°00′E, and latitudes 16°10′N and 21°30′N. The northern coastline of Vietnam surrounds the gulf to the west, China's Guangxi province to the north and China's Leizhou Peninsula and Hainan Island to the east (Minh et al., 2014). The total coastline length is about 800 km and 700 km for Vietnam and China, respectively (Thao, 2005). Tonkin is a shallow gulf, where the depth is <100 m. In this study, we focus only on the western part of the Tonkin Gulf (Fig. 1). It should be noted that the agreement had been signed between Vietnam and China in Beijing on 25th December 2000, in dealing with the delimitation of territorial boundary and fisheries cooperation (Thao, 2005). The Gulf of Tonkin has huge fossil fuel resources (Gao et al., 2013) (e.g., oil and natural gas) with approximately 2.3 billion tons of oil and 1.5 billion cubic meters of natural gas, respectively.

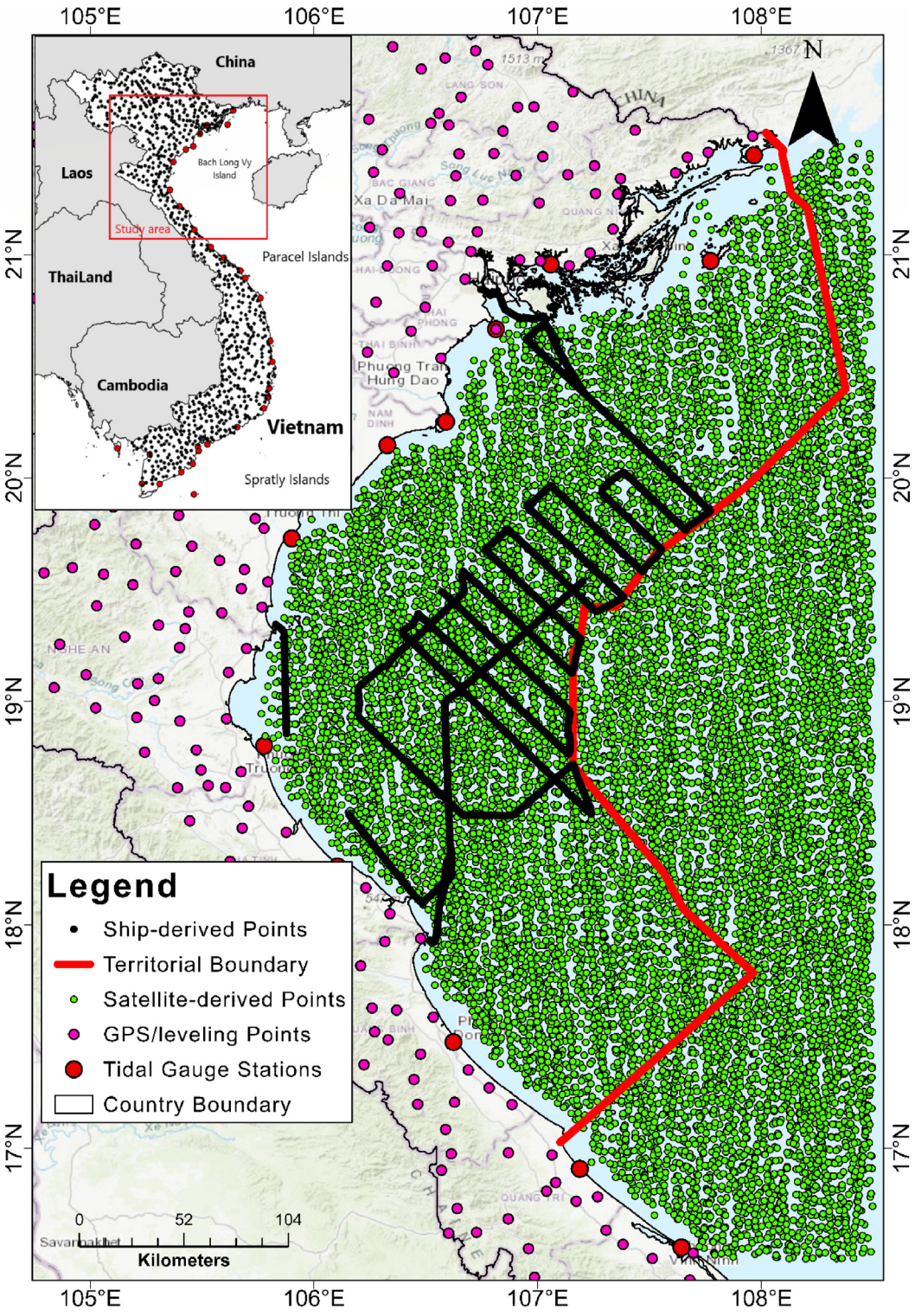

Fig. 1. Measurements on the Gulf of Tonkin area.

2.2. Data used

2.2.1. Satellite-derived measurement data

Cryosat-2, which was launched in 2010 by the International Space Company Kosmotras (ISC Kosmotras), is a radar altimetry mission, which was established and maintained by the European Space Agency (ESA). CryoSat-2 has been used to monitor variations in the thickness of the Earth's marine ice cover and continental ice sheets. Its primary objective is to measure the extent of thinning Arctic ice. CryoSat-2 is equipped with an advanced SAR/Interferometric Radar Altimeter-2 (SIRAL-2) and operates

in three modes: Low-Resolution Mode (LRM) i.e., pulse limited operation, Synthetic Aperture Radar (SAR), and SAR Interferometric (SARIn or SIN) burst modes over polar ice sheet boundaries, along coastal lines, some river basin and mountain areas (ESA-ESTEC, 2007, Tournadre et al., 2018). This satellite operates in a non-sun-synchronous polar orbit with the inclination of 92°. The repeated period is 369 days that provides equatorial distance between tracks of 7.5 km.

Saral/AltiKa, which was launched on 25 February 2013, is a jointed project between the Indian Space Agency and the French Space Agency. This is the first generation satellite equipped with a Ka-band altimeter for determining the height of ocean sea surface and the third-generation of ARGOS instrument for locating and collecting environmental data with an Argos transmitter (Aulicino et al., 2018, Verron et al., 2015). The satellite has been designed to operate over a 3-year lifetime and followed the sun-synchronous orbit (ERS-2 and ENVISAT satellites) on at the altitude of about 800 km with a 35-day repeat cycle (Abdalla, 2014). Saral/AltiKa finished its repetitive mission and begun the new phase named "SARAL Drifting Phase" (SARAL-DP) on 4 July 2016 (Verron et al., 2018). Saral/AltiKa satellite operated in exact repeat mission with 35-days cycle before July 2016. However, from 04th July 2016, Saral satellite has operated in the geodetic mission, and its observations are worldwide covering. Therefore, in this project, the Saral/AltiKa satellite observations from 2016 to 2018 were selected.

In this study, 6842 Cryosat-2 data points (SAR mode) from 27 cycles (from the 83rd cycle on 18 August 2016 to the 109th cycle on 22 September 2018) and 8823 Saral/AltiKa data points from 23 cycles (from the 36th cycle on 04 July 2016 to the 58th cycle on 15 January 2018) were used. These are shown as green points on Fig. 1. The sea surface height (*SSH*) (Chelton et al., 2001, Fu et al., 1994) in the Gulf of Tonkin were computed using:

$$SSH = \mathrm{H} - h - h_{cor} \tag{1}$$

where H is the height of the satellite over a reference ellipsoid, h is the height of the satellite over the current sea surface and h_{cor} are the corrections including: instrumental corrections; sea state bias corrections; ionospheric correction; tropospheric corrections (wet, dry); tides (ocean, earth, pole); inverse barometer. In this study, we used only SSH data that has been already preprocessed and provided by Centre National D'Etudes Spatiales via AVISO website (visit web page: https://www.aviso.altimetry.fr/home.html).

2.2.2. Marine gravity

In this study, a total of 58,989 gravity points, which were measured by a ship using the ZLS Dynamic gravity Meter, were used. These points were provided by the Ministry of Natural Resources & Environment of Vietnam (Nguyên Tính, 2012). The accuracy was around ± 1 mGal, whereas the cross-track spacing was about 15 km (the black points in Fig. 1). The details of the data used are described in Table 1.

2.2.3. GPS/leveling data

In order to select the best suitable Earth Geopotential Model for the study area, which can be used for determining gravity anomaly from satellite altimetry data, a total of 818 GPS/leveling points were used (the pink points in Fig. 1). These points have been measured using leveling as well as GPS methods.

2.2.4. Tidal gauge data

Data at 31 tidal gauge stations were used to find the best Mean Dynamic Topography (MDT) model for the study area. The tide-gauge observations had been monitored over 18.6 years, high accuracy GPS and leveling measurements had been used to determine locations and heights of these stations. These tidal gauge stations (the red points) are shown in Fig. 1.

3. Methodology

3.1. Computing the marine gravity anomaly using the Least-Squares Collocation method

The overall flow chart for computing the marine gravity anomaly using the LSC method is shown in Fig. 2. The detailed nomenclatures used in this figure are explained in the appendix.

3.2. Performing the remove the long-wavelength geoid height

The process of removing the long-wavelength geoid height ($\mathrm{N_{EIGEN}}$) was carried out using the following formulas (Hofmann-Wellenhof and Moritz, 2006):

$$N_{EIGEN} = \frac{GM}{\gamma r}\left[\sum_{n=2}^{N_{\max}}\left(\frac{a}{r}\right)^{n}\sum_{m=0}^{n}\left(\overline{C}_{n,m}\cos(m\lambda)+\overline{S}_{n,m}\sin(m\lambda)\right)\overline{P}_{n,m}(\sin\varphi)\right] \tag{2}$$

where GM: Earth's gravitational constant; r: distance from the point to the mass Earth's center; γ: normal gravity on the ellipsoidal surface; a: semi-major axis of reference ellipsoid; n, m: degree and order of spherical harmonic, respectively; $\mathrm{N_{max}}$: the maximum spherical harmonic degree ($\mathrm{N_{max}}$ = 2190 for EIGEN6C4 model); φ: geocentric latitude; λ: geocentric longitude (geodetic longitude); $\overline{C}_{n,m}, \overline{S}_{n,m}$: normalized gravitational coefficients; $\overline{P}_{nm}(sin\varphi')$: normalized associated Legendre function. The spherical harmonic coefficients ($\overline{C}_{n,m}, \overline{S}_{n,m}$) of the Global Geopotential Models (GGMs) are available at the International Centre for Global Earth Models (ICGEM, 2019).

Based on the accuracy assessment of Earth Gravitational Models using GNSS/leveling data in some countries (e.g., USA, Canada, Europe, Australia, Japan, and Brazil)

Table 1
The satellite-derived data and the ship-measured gravity data.

Data source	Coverage φ: latitude; λ: longitude	No. of points	Mean	Min Max
Cryosat-2 observation (SSH)	16.5° N < φ < 22.0° N 105.5° E < λ < 108.5° E	6842	−18.544 m	–23.709 m −10.361 m
Saral/AltiKa observation (SSH)	16.5° N < φ < 22.0° N 105.5° E < λ < 108.5° E	8823	−18.700 m	–23.768 m −10.056 m
Ship measurement (Gravity anomaly)	17.9° N < φ < 20.8° N 105.8° E < λ < 107.8° E	58,989	−30.99 mGal	−61.46 mGal +27.91 mGal
Geoid Height (GPS/leveling)		818	−14.636 m	–33.168 m +5.596 m

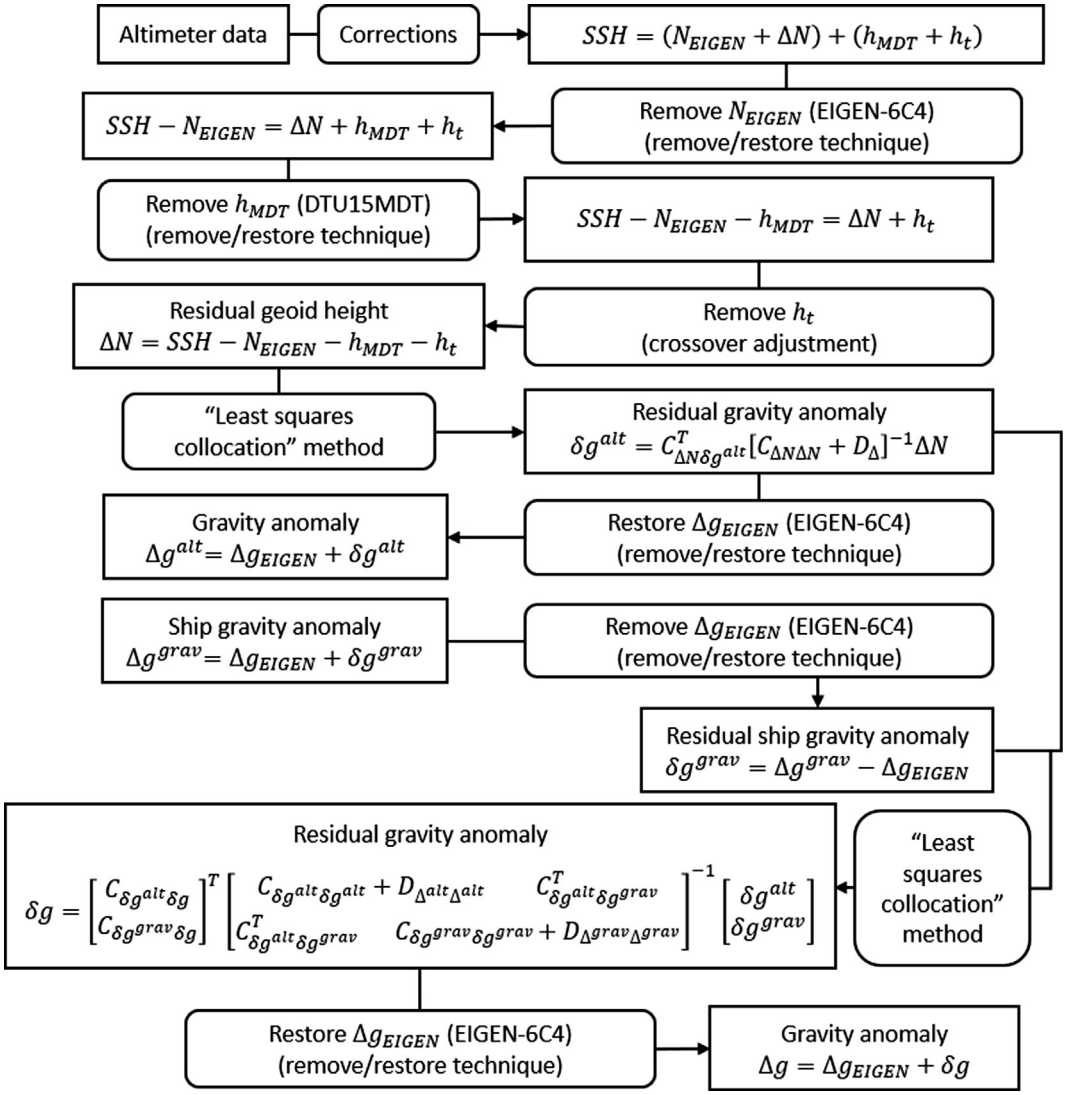

Fig. 2. Flow chart for computing the marine gravity anomaly using the LSC method (note: the same signal covariance functions are used for Δg^{grav}, Δg_{EIGEN} and δg^{grav}).

(ICGEM), 4 Earth Geopotential Models, whose spherical harmonics coefficients up to degree 2159 (SGG-UGM-1) and 2190 (EIGEN-6C4, GECO and EGM2008), have the highest precision (ICGEM, 2019). The geoid heights calculated from the four models were compared with the height values at 818 GPS/leveling points to choose the best suitable model for Vietnamese territory. The compared results are presented in Table 2.

It can be seen from Table 2, the standard deviation value between the EIGEN-6C4 model with GPS/leveling data in the Gulf of Tonkin is the smallest. It, therefore, shows that EIGEN-6C4 is the best Earth Geopotential Model in the

Table 2
The differences between the Earth Geopotential Models and the GPS/leveling data values in the Gulf of Tonkin. The statistics values were computed from the original data published in ICGEM (2019).

No.	Statistics (m)	SGG-UGM-1	EIGEN-6C4	GECO	EGM2008
1	Min	−0.202	+0.032	−0.035	−0.120
2	Max	+1.453	+1.453	+1.572	+1.688
3	Mean	+0.860	+0.901	+0.888	+0.815
4	Std. dev	±0.198	±0.193	±0.199	±0.292

study area. Therefore, EIGEN-6C4 has been selected as the reference model for the study area.

It should be noted that the EIGEN-6C4 was established by the GFZ Postdam in 2014 using the altimetric satellite data from DTU10 and DTU12, the terrestrial gravity data from EGM2008, and the satellite gravity data from GOCE, GRACE, and LAGOES. However, the altimetric satellite data used for this project were from 2016 to 2018; therefore, no correlation exists. According to Table 2, there is an offset of about 90 cm between geoid heights from GPS/leveling and the EIGEN model. This value exists because the reference height datum offset of Vietnam with the global system is 87 cm and had been used consistently in the WGS84 system.

The long-wavelength geoid heights calculated from Eq. (2) using the harmonic coefficients of the Earth Geopotential Model EIGEN-6C4 at 15,665 points of satellite altimetry Cryosat-2 and Saral/AltiKa are shown in Fig. 3a.

3.3. Removing the mean dynamic topography

In order to remove the mean dynamic topography (h_{MDT}) in the Gulf of Tonkin, five global mean dynamic topography models (e.g., DNSC08MDT, DTU10MDT, DTU12MDT, DTU13MDT, and DTU15MDT) were considered. These models had been mainly established based on the long period satellite-derived altimeter data or improvements from the previous models (Andersen et al., 2015, Andersen and Knudsen, 2009, Andersen and Knudsen, 2016). The mean dynamic topography (h_{MDT}) is the average value of the difference between the mean sea surface (h_{MSS}) and the geoid heights (N_{EIGEN}) over many years (Andersen and Knudsen, 2009, Rio and Hernandez, 2004):

$$h_{MDT} = h_{MSS} - N_{EIGEN} \tag{3}$$

Based on 31 tidal gauge stations data, the mean dynamic topography heights over Vietnam area (h_{MDT_VN}) were calculated. The mean dynamic topography height at these

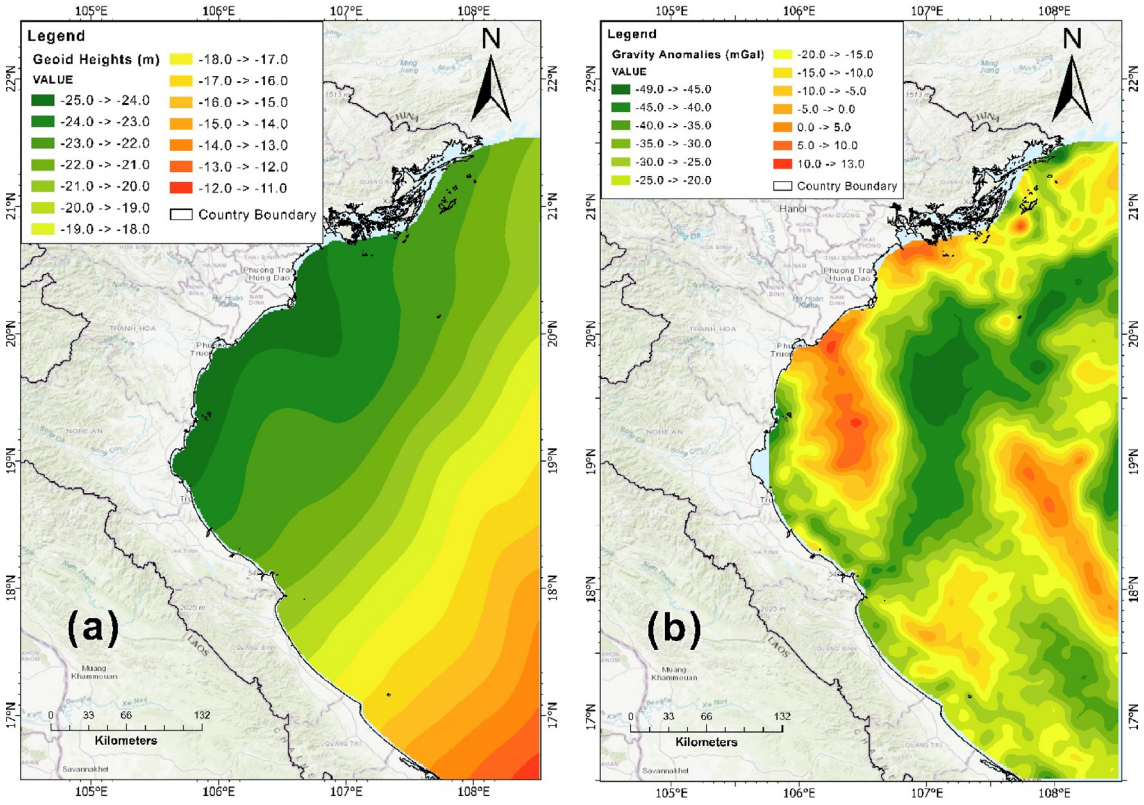

Fig. 3. The maps of geoid heights(N_{EIGEN}) (a) and gravity anomalies (Δg_{EIGEN}) (b).

tidal gauge stations was also computed using five global mean dynamic topography models(h_{MDT_DTU}). As a result, there were two values at these 31 tide gauge stations, the first one calculated from tidal gauge stations and another one calculated from global MDT. The differences between these values are shown in Table 3.

The data in Table 4 has been calculated following by these formulas:

$$\delta^{i}_{h_{MDT}} = h^{i}_{h_{MDT\_VN}} - h^{i}_{h_{MDT\_DTU}} \quad (4)$$

$$\delta^{ave}_{h_{MDT}} = \frac{1}{n}\sum_{i=1}^{n}\delta^{i}_{h_{MDT}} \quad (5)$$

$$\sigma_{h_{MDT}} = \sqrt{\frac{1}{n-1}\sum_{i=1}^{n}\left(\delta^{i}_{h_{MDT}} - \delta^{ave}_{h_{MDT}}\right)^{2}} \quad (6)$$

where: $h^{i}_{h_{MDT\_VN}}$ and $h^{i}_{h_{MDT\_DTU}}$ are the mean dynamic topography computed from the i^{th} Vietnamese tidal gauge station and the MDT model, respectively; $\sigma_{h_{MDT}}$ is the standard deviation, and n is the total of measured points (the range is from 1 to 31).

The experimental results in Table 4 showed that DTU15MDT was the best suitable model for the study area. Therefore, the DTU15MDT model with the $1'\times1'$ gridded resolution had been chosen to calculate the mean dynamic topography(h_{MDT}).

3.4. Removing the time-varying sea-surface topography using the crossover adjustment method

This step aims to remove the time-varying sea-surface topography value (h_t) (see Fig. 2). The surface height difference (dH) at each crossover points can be calculated from the north-going track (h_i) and the south-going track (h_j) by the following formula (Andersen, 2013):

$$dH_{ij} = h_i - h_j \quad (7)$$

According to Fig. 2, the time-varying sea-surface topography value needs to be removed to calculate gravity anomaly from altimetry satellite data. In order to remove this value, we have modeled it into bias and tilt and, after that, the relationship between this value and bias and tilt had

Table 3
The accuracy of MDT models on the Vietnam sea area.

No.	Name of tidal stations	The difference between the two mean dynamic topography heights				
		$\delta_{h_{DNSC08MDT}}$	$\delta_{h_{DTU10MDT}}$	$\delta_{h_{DTU12MDT}}$	$\delta_{h_{DTU13MDT}}$	$\delta_{h_{DTU15MDT}}$
1	Co To	−0.7075	−0.9065	−0.9965	−1.0205	−0.9685
2	Hon Dau	−1.0308	−0.8918	−1.1378	−1.1658	−1.1478
3	Hon Ngu	−1.1816	−1.2116	−1.1456	−1.1676	−1.0826
4	Tien Sa-Son Tra	−0.3499	−1.0489	−1.0779	−1.0849	−1.0169
5	Quy Nhon	−0.8267	−1.1607	−1.0167	−1.0387	−0.9627
6	Nha Trang	−0.9478	−1.2028	−1.0928	−1.1088	−1.0158
7	Vung Tau	−1.1429	−1.3579	−1.2519	−1.2459	−1.1749
8	Phu Quoc	−1.1659	−1.3129	−1.3269	−1.3569	−1.2929
9	Con Dao	−1.1017	−1.1317	−1.1857	−1.1767	−1.1197
10	Mui Ngoc	−1.1690	−1.0750	−1.0980	−1.1300	−1.0460
11	Bai Chay	−0.9325	−0.9205	−1.1625	−1.1925	−1.1655
12	Ba Lat	−0.8392	−0.7282	−0.9492	−0.9772	−0.9462
13	Cua Day	−0.7973	−0.6413	−0.8463	−0.8733	−0.8343
14	Hoang Tan	−0.4647	−1.0107	−1.1547	−1.1787	−1.0997
15	Cam Nhuong	−1.0361	−1.2041	−1.0601	−1.0831	−1.0011
16	Dong Hoi	−0.9078	−1.2938	−1.2328	−1.2538	−1.1528
17	Cua Viet	−0.8743	−1.3613	−1.4283	−1.4443	−1.3613
18	Thuan An	−0.8256	−1.2466	−1.3406	−1.3516	−1.2826
19	Cua Dai	−0.7251	−1.1421	−1.1221	−1.1291	−1.0531
20	Cang Sa Ky	−0.9387	−1.0847	−0.9517	−0.9607	−0.8847
21	Tuy Hoa	−0.9722	−1.3662	−1.2682	−1.2912	−1.2082
22	Cam Ranh	−0.7250	−1.1070	−0.9960	−1.0060	−0.9150
23	Phan Rang	−1.1622	−1.2242	−1.1182	−1.1242	−1.0412
24	Phan Thiet	−0.7306	−1.0926	−0.9876	−0.9826	−0.9116
25	Vam Kenh	−0.7999	−0.9529	−0.8709	−0.8689	−0.7939
26	Binh Dai	−1.0990	−1.1900	−1.1170	−1.1140	−1.0400
27	Tra Vinh	−1.1192	−1.0832	−1.0722	−1.0682	−0.9942
28	Tran De	−0.9343	−1.0163	−1.0473	−1.0463	−0.9693
29	Ghanh Hao	−0.8845	−1.0365	−1.0895	−1.0905	−1.0165
30	Rach Gia	−0.5551	−1.0691	−1.1341	−1.1571	−1.0901
31	Hon Da Bac	−0.9345	−1.0235	−1.0965	−1.0985	−1.0275
Min (m)		−1.182	−1.366	−1.428	−1.444	−1.361
Max (m)		−0.350	−0.641	−0.846	−0.869	−0.794
Mean (m)		−0.899	−1.100	−1.109	−1.122	−1.052
Std. dev (m)		±0.208	±0.172	±0.131	±0.132	±0.131

Table 4
Results of the empirical covariance and analytic covariance using the satellite-derived gravity anomaly data.

No.	ψ_i(degree)	Covariance, m^2		No.	ψ_i(degree)	Covariance, m^2	
		Empirical covariance	Analytic covariance			Empirical covariance	Analytic covariance
1	0.000	0.0368	0.0346	11	1.667	0.0031	0.0050
2	0.167	0.0283	0.0296	12	1.833	0.0012	0.0007
3	0.333	0.0161	0.0170	13	2.000	−0.0001	−0.0030
4	0.500	0.0024	0.0021	14	2.167	0.0001	−0.0042
5	0.667	−0.0075	−0.0089	15	2.333	0.0010	−0.0027
6	0.833	−0.0111	−0.0123	16	2.500	0.0006	−0.0001
7	1.000	−0.0079	−0.0087	17	2.667	−0.0006	0.0019
8	1.167	−0.0022	−0.0014	18	2.833	−0.0014	0.0022
9	1.333	0.0027	0.0049	19	3.000	−0.0022	0.0011
10	1.500	0.0045	0.0072				

been built. The crossover adjustment method, finally, had been employed to estimate bias and tilt and remove h_t (Andersen, 2013).

3.5. Determining marine gravity anomalies using the Least-Squares Collocation method

To calculate gravity anomaly from satellite altimetry data using Least-Squares Collocation, we have to determine the cross-covariance between residual gravity anomaly and residual geoid height. However, only the latter is available. For this reason, in this work, a method proposed by Tscherning and Rapp (1974) was used (Eqs. (9) and (10)). In this analysis, the fitting processing was carried out using the CovFit module in the Gravsoft program (Forsberg and Tscherning, 2008).

According to the LSC method, the residual gravity anomaly at the specific P (computational point of gravity anomaly) is given by the following formula (Sansò and Sideris, 2013, Tscherning and Rapp, 1974):

$$\delta g_P = C^T_{\Delta N \delta g_P}[C_{\Delta N \Delta N} + D_\Delta]^{-1}\Delta N \tag{8}$$

$$C_{\Delta N_i \delta g_P} = \frac{a}{\gamma_i}\sum_{n=2}^{N} d_n \frac{n-1}{r_P}\left(\frac{R^2}{r_i r_P}\right)^{n+1} P_n cos\psi + \frac{1}{\gamma_i}\sum_{n=N+1}^{\infty} \times \frac{A}{(n-2)(n+b)}\frac{1}{r_P}\left(\frac{R_B^2}{r_i r_P}\right)^{n+1} P_n cos\psi \tag{9}$$

$$C_{\Delta N_i \Delta N_i} = a\sum_{n=2}^{N} d_n \frac{1}{\gamma_i \gamma_j}\left(\frac{R^2}{r_i r_j}\right)^{n+1} P_n cos\psi + \sum_{n=N+1}^{\infty} \times \frac{A}{(n-2)(n+b)}\frac{1}{\gamma_i \gamma_j}\left(\frac{R_B^2}{r_i r_j}\right)^{n+1} P_n cos\psi \tag{10}$$

$$D_\Delta = \begin{bmatrix} D_{1,1}D_{1,2}\cdots D_{1,n} \\ D_{2,1}D_{2,2}\cdots D_{2,n} \\ \cdots\cdots\cdots\cdots \\ D_{n,1}D_{n,2}\cdots D_{n,n} \end{bmatrix} \tag{11}$$

It should be noted that the off-diagonal elements of the D-matrix are approximate zero; however, the determination of these values is impossible. In this research, we used zero values for the elements.

The accuracy is assessed using the following equation:

$$\sigma^2_{\delta g_P} = C_{\delta g_P \delta g_P} - C^T_{\Delta N \delta g_P}[C_{\Delta N \Delta N} + D_\Delta]^{-1} C_{\Delta N \delta g_P} \tag{12}$$

where C: covariance function;D_Δ: error covariance matrix; ΔN: residual geoid height; $P_n(cos\psi)$: Legendre polynomial of degree n; ψ: the spherical distance between two points; R: the radius of the Earth; a: additional parameters (a = 28.3622); d_n: variance of coefficients to degree N; b: an integer, chosen as 4; A: is a constant; R_B: the radius of the Bjerhammar-sphere; N: the degree value used in the EGM96 model.

The parameters a, d_n, N, A, R_B are determined by fitting the analytic covariance function with the values of an empirical covariance function using the following formula:

$$\widehat{C}_{\Delta N}(\psi_i) = \frac{1}{m_i}\sum_{n=1}^{m_i}[\Delta N_P \Delta N_{P'}]_n \tag{13}$$

where m_i is the total of pairs of points; P and P' are all the points that have spherical distances ψ, which satisfy the condition:

$$\psi_i - \frac{\Delta\psi}{2} \le \psi \le \psi_i + \frac{\Delta\psi}{2} \tag{14}$$

These parameters a, d_n, N, A, R_B have been used as input data for formula (9) and (10) to calculate covariance values, then it has been employed for formula (8) to compute gravity anomaly.

3.6. Fitting satellite-derived gravity anomalies with the ship-measured gravity anomalies using the Least-Squares Collocation method

The residual gravity anomaly value using the LSC method at the point P is given by the formula (Sansò and Sideris, 2013):

Table 5
Statistics of the residual geoid height and the satellite-derived marine gravity anomalies on the Gulf of Tonkin.

Type of data	Coverage (φ: latitude; λ: longitude)	No. of points	Average (mGal)	Min Max (mGal)	Std. dev (m)
Residual geoid height	16.5°N < φ < 22.0°N 105.5°E < λ < 108.5°E	15,665	+0.145	−0.611 +0.796	±0.194
Gravity anomalies	16.5°N < φ < 22.0°N 105.5°E < λ < 108.5°E	15,665	−24.74	−63.22 +15.09	

Table 6
The empirical and analytic covariance results of the fitting satellite-derived anomalies and the ship-measured gravity anomalies.

No.	ψ_i(degree)	Covariance, mGal^2		No.	ψ_i(degree)	Covariance, mGal^2	
		Empirical covariance	Analytic covariance			Empirical covariance	Analytic covariance
1	0.000	75.918	74.020	11	1.667	6.940	9.615
2	0.167	61.601	62.773	12	1.833	1.876	−1.219
3	0.333	33.351	34.505	13	2.000	−1.586	−9.087
4	0.500	2.450	1.799	14	2.167	−1.690	−9.956
5	0.667	−19.264	−21.320	15	2.333	−0.069	−4.808
6	0.833	−25.124	−27.039	16	2.500	0.540	2.051
7	1.000	−16.436	−16.935	17	2.667	0.574	6.056
8	1.167	−2.796	0.140	18	2.833	0.192	5.361
9	1.333	7.670	13.414	19	3.000	−1.225	1.437
10	1.500	10.762	16.483				

Table 7
Comparison of the satellite-derived gravity and fitted gravity anomalies with the ship-measured gravity anomalies.

Note	Coverage (φ: latitude; λ: longitude)	No. of points	Mean (mGal)	Std. dev (mGal)	RMSD (mGal)	Min, Max (mGal)
Satellite-derived gravity anomalies with the ship-measured gravity anomalies	16.5°N < φ < 22°N 105.5° E < λ < 108.5°E	56,978	+2.06	±3.36	±3.94	−38.00 +44.38
Fitted gravity anomalies with the ship-measured gravity anomalies	17.9°N < φ < 20.8° N 105.8° E < λ < 107.8°E	56,978	+0.04	±2.63	±2.63	−46.01 +36.08
DTU10GRAV	16.5°N < φ < 22°N 105.5° E < λ < 108.5°E	56,978	+2.98	±5.80	±6.52	−44.17 +40.02
DTU13GRAV	16.5°N < φ < 22°N 105.5° E < λ < 108.5°E	56,978	+2.94	±5.73	±6.44	−44.13 +40.16
DTU15GRAV	16.5°N < φ < 22°N 105.5° E < λ < 108.5°E	56,978	+3.18	±5.63	±6.47	−43.99 +40.30

$$\delta g_P = \begin{bmatrix} C_{\delta g^{alt}\delta g_P} \\ C_{\delta g^{grav}\delta g_P} \end{bmatrix}^T \begin{bmatrix} C_{\delta g^{alt}\delta g^{alt}} + D_{\Delta^{alt}\Delta^{alt}} C^T_{\delta g^{alt}\delta g^{grav}} \\ C^T_{\delta g^{alt}\delta g^{grav}} C_{\delta g^{grav}\delta g^{grav}} + D_{\Delta^{grav}\Delta^{grav}} \end{bmatrix}^{-1} \begin{bmatrix} \delta g^{alt} \\ \delta g^{grav} \end{bmatrix} \tag{15}$$

where δ_k^{alt} and δ_m^{shg} are the number of the residual satellite-derived and ship-measured gravity anomalies, respectively.

$$C_{\delta g_i \delta g_j} = a \sum_{n=2}^{N} d_n \frac{(n-1)^2}{r_i r_j} \left(\frac{R^2}{r_i r_j}\right)^{n+1} P_n cos\psi + \sum_{n=N+1}^{\infty} \times \frac{A}{(n-2)(n+b)} \frac{n-1}{r_i r_j} \left(\frac{R_B^2}{r_i r_j}\right)^{n+1} P_n cos\psi \tag{16}$$

$$C^T_{\delta g \delta g_P} = \left[C^T_{\delta g_1 \delta g_P} C^T_{\delta g_2 \delta g_P} \cdots C^T_{\delta g_t \delta g_P} \right] \tag{17}$$

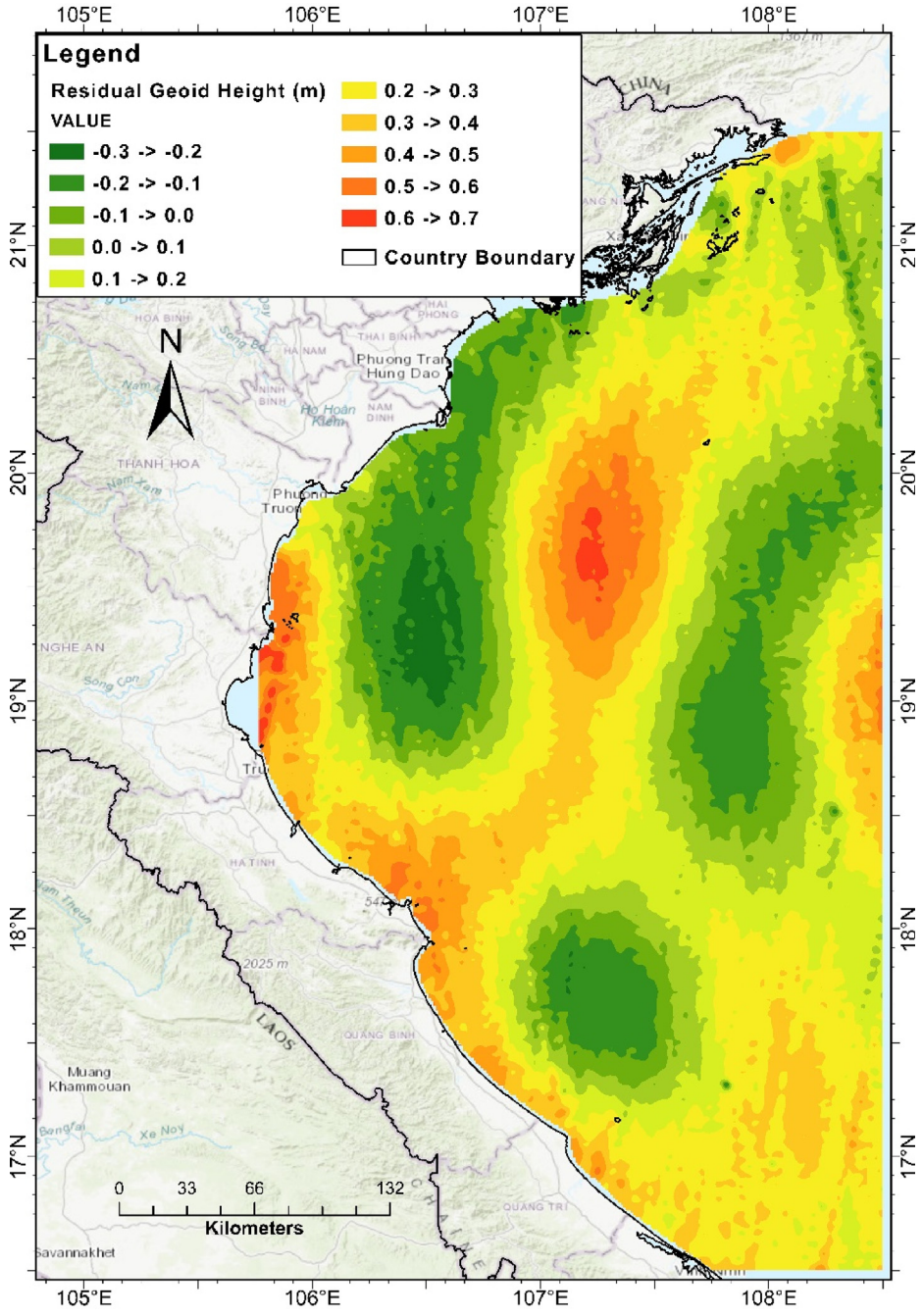

Fig. 4. The residual geoid height in the Gulf of Tonkin.

$$C_{\delta g \delta g} = \begin{bmatrix} C_{\delta g_1 \delta g_1} C_{\delta g_1 \delta g_2} \cdots C_{\delta g_1 \delta g_t} \\ C_{\delta g_2 \delta g_1} C_{\delta g_2 \delta g_2} \cdots C_{\delta g_2 \delta g_t} \\ \cdots\cdots\cdots\cdots \\ C_{\delta g_t \delta g_1} C_{\delta g_t \delta g_2} \cdots C_{\delta g_t \delta g_t} \end{bmatrix} \quad (18)$$

$$D_{\Delta\Delta} = \begin{bmatrix} D_{\Delta_1\Delta_1} D_{\Delta_1\Delta_2} \cdots D_{\Delta_1\Delta_t} \\ D_{\Delta_2\Delta_1} D_{\Delta_2\Delta_2} \cdots D_{\Delta_2\Delta_t} \\ \cdots\cdots\cdots\cdots \\ D_{\Delta_t\Delta_1} D_{\Delta_t\Delta_2} \cdots D_{\Delta_t\Delta_t} \end{bmatrix} \quad (19)$$

In the formulas (17) to (19): t = k for satellite-derived gravity anomaly, and t = m for ship-measured gravity anomaly. The on-diagonal elements of the D-matrix of ship-borne and altimetric gravity anomaly are determined based on ship-borne measuring accuracy and altimetric gravity anomaly (when comparing with direct gravity accuracy), respectively. The off-diagonal elements of the D-matrix are zero.

3.7. Restoring the long-wavelength gravity anomaly

The process of removing the long-wavelength geoid height (N_{EIGEN}) and restoring the long-wavelength gravity anomaly (Δg_{EIGEN}) from the spherical harmonic coeffi-

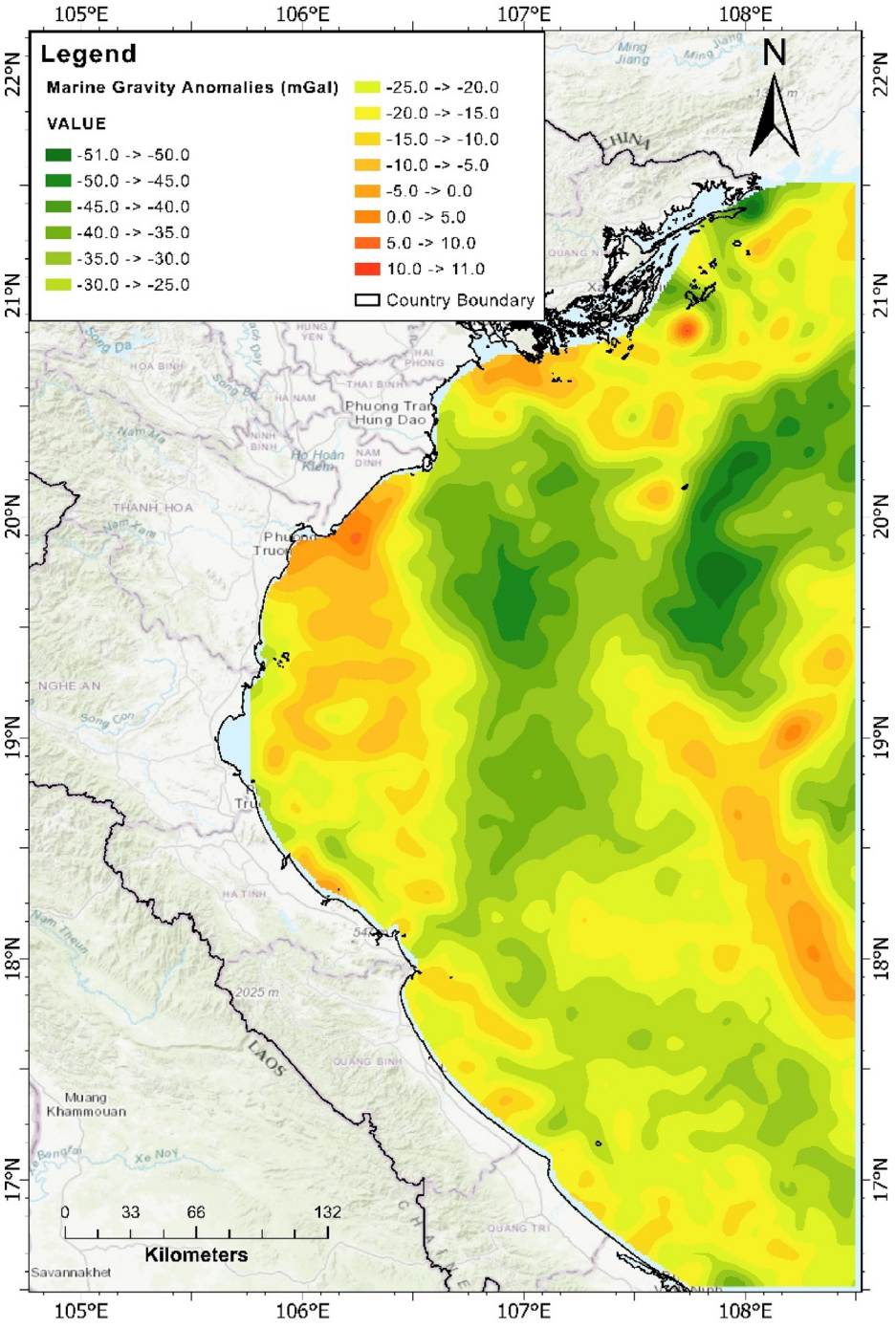

Fig. 5. The marine gravity anomalies calculated from Cryosat-2 and Saral/AltiKa data.

cients were carried out using the following formulas (Hofmann-Wellenhof and Moritz, 2006):

$$\Delta g_{EIGEN} = \frac{GM}{r^2}\left[\sum_{n=2}^{N_{max}}\left(\frac{a}{r}\right)^n (n-1)\sum_{m=0}^{n}\left(\overline{C}_{nm}cos(m\lambda) + \overline{S}_{nm}sin(m\lambda)\right)\overline{P}_{nm}(sin\varphi)\right] \quad (20)$$

The detailed nomenclatures used in Eq. (20) are explained in Eq. (2).

Gravity anomalies calculated from Eq. (20) using the harmonic coefficients of the Earth Geopotential Model EIGEN-6C4 at 15,665 grid points of satellite altimetry Cryosat-2 (grid 6842 points) and Saral/AltiKa (8823 grid points) are shown in Fig. 3b.

4. Results

4.1. Marine gravity anomalies from Cryosat-2 and Saral/AltiKa satellite altimeter data

After removing the long-wavelength geoid height (EIGEN-6C4) and the mean dynamic topography

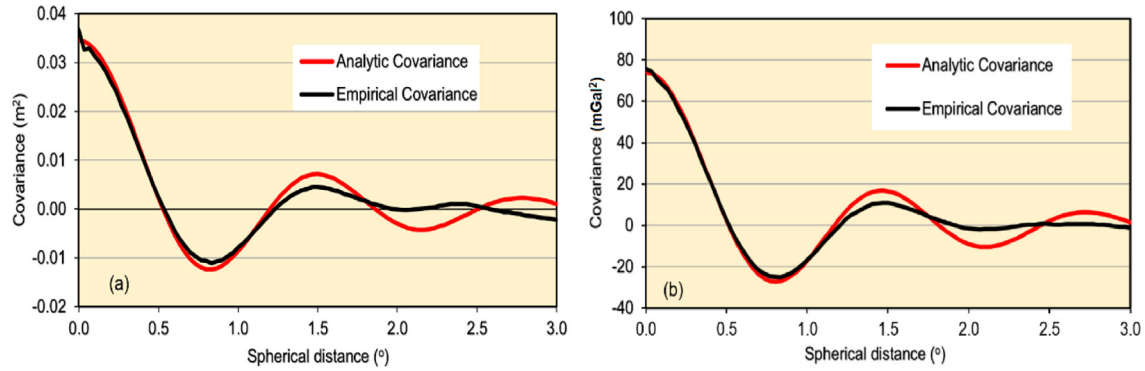

Fig. 6. (a) The covariance function of residual geoid heights and (b) the covariance function of the total gravity anomaly signal from a combination of altimetric and ship data.

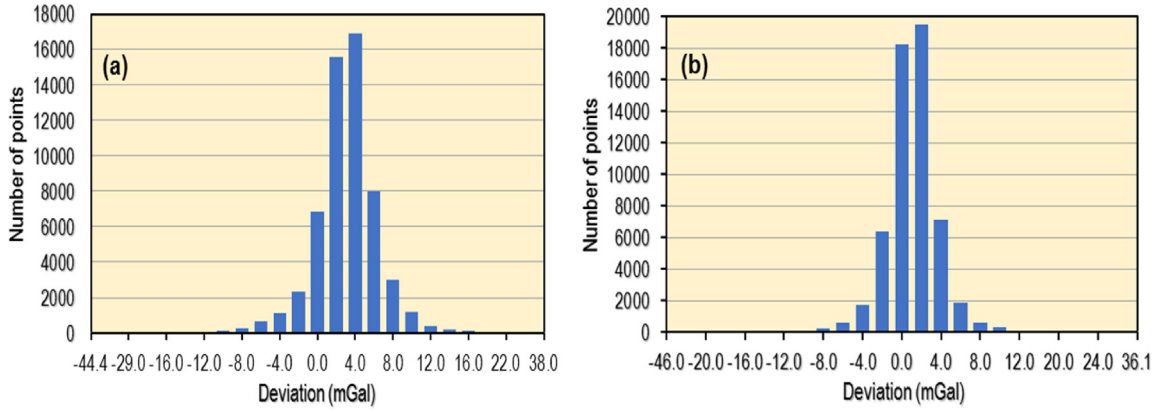

Fig. 7. The deviation histogram for differences between satellite-derived gravity anomalies and ship-measured gravity anomalies before (a) and after (b) fitted.

(DTU15MDT), the crossover adjustment method was carried out for Cryosat-2 and Saral/AltiKa satellite altimetry data to remove the time-varying sea-surface topography h_t and obtain residual geoid height (Fig. 4).

The result of the residual geoid height in the Gulf of Tonkin is shown in Table 4.

In order to calculate the residual gravity anomaly from the residual geoid height using the LSC method, the determination of the parameters of the analytic covariance function is essential (Eq. (13)). The parameters in Eqs. (8)–(10), (16) are calculated using the EmpCov, the Covfit, and the Geocol modules of the GRAVSOFT package (Forsberg and Tscherning, 2008). The results of empirical covariance and analytic covariance are shown in Table 4 and Fig. 6a. When the parameters of the analytic covariance function get: $N = 310; a = 28.3622; R_B - R = -1.0\ km; A = 0.0007657(m/s)^4$ (see Section 3.5), the variance of gravity anomaly is57.16 $mGal^2$.

The marine gravity anomalies using Cryosat-2 and Saral/AltiKa satellite altimeter data on the Gulf of Tonkin are illustrated in Table 5 and Fig. 5. From Fig. 5, and Fig. 3b, the gravity field has been presented clearly when satellite altimeter data had been applied.

4.2. Fitting Cryosat-2 and Saral/AltiKa satellite-derived with ship-measured gravity anomalies

In order to fit the satellite-derived gravity anomalies with ship-measured gravity anomalies as well as assessing the accuracy, 58,989 points were used and separated into two subsets:

- The first one, including 2011 points, was used for fitting. These points were selected equilateral in the study area, and the distance between them was about 1 km along ship tracks.
- The second subset consisting of the remaining 56,978 points, and was used for assessing the marine gravity anomaly accuracy.

Satellite-derived gravity anomaly was fitted with ship-measured data following two steps: (1) a system differences were removed by using satellite-calculated gravity anomaly

minus system error (+2.06 mGal); (2) satellite-derived gravity anomaly and ship-calculated gravity anomaly were fitted together employing Collocation method.

The empirical covariance and the analytic covariance values in Table 4 were derived using the satellite-derived gravity anomaly data only. Besides, the EIGEN-6C4 model has been used to remove and restore the long-wavelength gravity anomalies. Then, these covariance values were recomputed using both the satellite-derived gravity anomaly and ship-measured gravity anomaly data. The result is shown in Table 6 and Fig. 6b. The parameters used are $N = 310$, $a = 36, R_B - R = -0.99999\ km$, and $A = 0.0007658\ (m/s)^4$. The variance of gravity anomaly is 74.02 $mGal^2$.

4.3. Validation and Comparison of the result

a. Comparison of gravity anomaly computed from satellite altimetric and ship-borne data

After calculating the marine gravity anomalies from the integration of satellite data (see Section 4.1), these values were compared with the 56,978 ship-measured points at the second subset (see Section 4.2). Thus, each point has two values: the first value is direct gravity anomaly and the second is satellite-derived gravity anomaly. The differences between these values are in Table 7.

Root mean squares of the differences (RMSD) between satellite-derived and ship-derived gravity anomalies were estimated as (Ruiz Etcheverry et al., 2015):

$$RMSD = \sqrt{\frac{1}{n}\sum_{i=1}^{n}\left(\Delta g^i_{alt} - \Delta g^i_{grav}\right)^2} \quad (21)$$

where $\Delta g^i_{alt}, \Delta g^i_{grav}$ are satellite-derived and ship-derived gravity anomalies, respectively.

It could be seen that the standard deviation is ± 3.36 mGal, indicating good accuracy and follow the standard normal distribution rule. However, a system error has existed because the mean value is quite high, about + 2.06 mGal.

b. Comparison of gravity anomaly computed from combining satellite altimetry and ship-borne gravity data with ship-borne gravity data

Gravity anomaly calculated from satellite altimetry data after fitting with 2011 ship-measured points at the first subset has been compared with 56,978 ship-measured gravity points at the second subset. The comparison results are showed in Table 7.

It can be seen that the accuracy of gravity anomaly is improved. The standard deviation was reduced from ±3.36 mGal to ±2.63 mGal; the mean difference was reduced from +2.06 mGal to +0.04 mGal. The system error was nearly zero, as well as RMSD (from ±3.94 mGal to ±2.63 mGal). The results in Fig. 7 show that the gravity anomaly difference follows the standard normal distribution rule.

It is clear that the satellite-based gravity data are usually deteriorated in complex regions, i.e., regions near islands and coastal zones as this study area; therefore, the global gravity models are not always feasible (Shen et al., 2017). Compared to other works, where the accuracy (root mean squares of the discrepancies) between the satellite-derived gravity anomalies and the shipboard-measured gravity anomalies is 5.217 mGal in the southern coast of Taiwan, ±5.986 mGal in South China Sea Basin, ±5.647 mGal in around the Okinawa areas, and ±8.279 mGal in around the Philippine islands (Shen et al., 2017), ±3.91 mGal in the Northwest Atlantic Ocean (Andersen et al., 2010), ±2.0 – ±4.0 mGal in the Gulf of Mexico (Sandwell and Smith, 2009a), ~±4.0 mGal in the Gulf Stream (Andersen et al., 2010), and ~±8.5 mGal in the East Vietnam Sea and adjacent areas (Dung et al., 2019), the obtained result in this research is somewhat better. In fact, the accuracy of the marine gravity anomaly depends on various factors, i.e., range precision and sampling rate (Sandwell et al., 2019), but in the Gulf of Tonkin, the accuracy is influenced by the tide corrections. However, in this study, tide corrections have not used for estimating marine gravity anomaly in the Gulf of Tonkin and this makes a limitation of our study. Using 31 tidal stations to estimate and chose the best suitable MDT model in the study area, the accuracy of the marine gravity anomaly in the Gulf of Tonkin was improved. Besides, fitting satellite-derived gravity anomaly with ship-borne gravity data has improved gravity anomaly estimation accuracy.

In this study, we also estimated the accuracy of DTU10-GRAV, DTU13GRAV, DTU15GRAV models in the Gulf of Tonkin by comparing with direct gravity data (see Table 7). In the Gulf of Tonkin, the standard deviations between gravity anomaly and ship-based values of DTU10-GRAV, DTU13GRAV, DTU15GRAV models in the Gulf of Tonkin are ±5.80 mGal, ±5.73 mGal and ±5.63 mGal with system error values are +2.98 mGal, +2.94 mGal and +3.18 mGal, respectively. Comparing with the results in our study, marine gravity anomaly accuracy in the study area was higher than available result. Specifically, the accuracy of gravity anomaly was ±3.36 mGal before fitting, the system error was removed and the accuracy was improved about ±2.63 mGal after satellite-derived gravity anomaly fitted with ship-calculated gravity anomaly.

5. Concluding remarks

Determination of the marine gravity anomaly with high resolution and accuracy is crucial for various applications. This study applied the LSC method for estimating marine gravity anomalies with 2′×2′ resolution grid for the Gulf of Tonkin (Vietnam) using integrated satellite and terrestrial data. In this regard, Cryosat-2 and Saral/AltiKa satellite altimeter data, GPS/leveling, and tidal gauge of 31 tidal stations were used. Also, the quality of the derived marine gravity anomaly was assessed using the gravity points measured by boat. Thus, in this research, the main focuses are:

- Selection of the suitable EGM and MDT models for the study area using the local GPS/leveling and tidal gauge data.
- Using the combined Cryosat-2 and Saral/AltiKa data to enhance the data density.
- Investigating how much the accuracy can be improved when additional measured data (ship, GPS/leveling, and tide gauge data) used together with the satellite altimeter data for the marine gravity anomaly.
- Applications of the remove-restore technique, the cross-over adjustment algorithm, and the LSC method to determine marine gravity anomaly in the Gulf of Tonkin of Vietnam.

Based on the finding of this study, some conclusions are given below:

- Based on the GPS/leveling and the tidal gauges station data, the EIGEN6C4 and DTU15MDT are the most suitable models that should be used for the determination of marine gravity anomalies the Gulf of Tonkin.
- The limited Cryosat-2 and Saral/AltiKa satellite altimeter data, EIGEN6C4, and DTU15MDT models can help to derive the marine gravity anomaly with the good accuracy (±3.36 mGal for the Gulf of Tonkin of Vietnam). Additionally, the accuracy is increased significantly with the use of ship-derived gravity anomaly points (reach to ± 2.63 mGal in the study area).
- The least-squares collocation is an effective and robust method for handling combined data for determining marine gravity anomaly. Combination of the Cryosat-2 and Saral/AltiKa satellite altimeter is useful for the determination of marine gravity anomalies.
- The result of this work is useful for geodetic and geophysical applications in the Gulf of Tonkin region.
- Future works could focus on investigating other methods and algorithms for determining gravity anomaly in the near-shore regions, especially coastal regions.

CRediT authorship contribution statement

Van-Sang Nguyen: Data collection and processing, Methodology, and Writing the original draft manuscript. **Van-Tuyen Pham:** Data colection and processing, Methodology, and Writing the original draft manuscript. **Lam Van Nguyen:** Writing the original draft manuscript, Methodology. **Ole Baltazar Andersen:** Methodology, Software, Data, and Review and editing. **Rene Forsberg:** Methodology, Software. **Dieu Tien Bui:** Methodology and Review and editing.

Acknowledgment

The authors would like to thank the Union of Geology and Mineral Resources, Department of Geology and Minerals of Vietnam for providing 58989 ship-measured gravity points, these data belong to the project "*The investigation of geological, geodynamic and mineral characteristics, environmental geology and geological hazard prediction in Vietnam Sea regions*" (Vu et al., 2009) in the category of projects under decision N0. 47/2006/QD-TTg on March 01, 2006 of the Vietnamese Prime Minister. We would like to thank Assoc. Prof. Dr. Sc. Minh-Hoa Ha at Vietnam Institute of Geodesy and Cartography (VIGAC) for providing the data at 31 tide gauge stations along the coastal area of Vietnam as well as Prof. Dr. Sc. Hoang-Lan Pham at Hanoi University of Mining and Geology for providing the 818 GPS/leveling data.

Appendix.

Nomenclature	Description
SSH	Sea Surface Height
N_{EIGEN}	The long-wavelength geoid height calculated from EIGEN-6C4 model
ΔN	The residual geoid height (calculated by equation: $\Delta N = SSH - N_{EIGEN} - h_{MDT} - h_t$)
N	The geoid height
h_{MDT}, h_t	The Mean Dynamic Topography, time-varying sea-surface topography respectively
h_{MSS}	The Mean Sea Surface
$\delta g^{alt}, \delta g^{grav}$	The residual gravity anomaly calculated from satellite-derived and ship-measured gravity data respectively
$\Delta g^{alt}, \Delta g^{grav}$	The long-wavelength gravity anomaly calculated from satellite-derived and ship-measured gravity data respectively
C^T	The transposition covariance function
D_Δ	The covariance matrix of error
Δg_{EIGEN}	The long-wavelength gravity anomaly calculated from EIGEN-6C4 model

References

Abdalla, S., 2014. Calibration of SARAL/AltiKa wind speed. IEEE Geosci. Remote Sens. Lett. 11, 1121–1123.

Andersen, O., Knudsen, P., Kenyon, S., Factor, J., Holmes, S., 2013. The DTU13 Global marine gravity field—first evaluation. Ocean Surface Topography Science Team Meeting, Boulder, Colorado.

Andersen, O., Knudsen, P., Stenseng, L., 2015. The DTU13 MSS (Mean Sea Surface) and MDT (Mean Dynamic Topography) from 20 Years of Satellite Altimetry.

Andersen, O.B., 2013. Marine gravity and geoid from satellite altimetry. In: Sansò, F., Sideris, M.G. (Eds.), Geoid Determination: Theory and Methods. Springer, Berlin Heidelberg, Berlin, Heidelberg, pp. 401–451.

Andersen, O.B., Knudsen, P., 2009. DNSC08 mean sea surface and mean dynamic topography models. J. Geophys. Res. Oceans 114.

Andersen, O.B., Knudsen, P., 2016. Deriving the DTU15 Global high resolution marine gravity field from satellite altimetry.

Andersen, O.B., Knudsen, P., Berry, P.A., 2010. The DNSC08GRA global marine gravity field from double retracked satellite altimetry. J. Geod. 84, 191–199.

Aulicino, G., Cotroneo, Y., Ruiz, S., et al., 2018. Monitoring the Algerian Basin through glider observations, satellite altimetry and numerical simulations along a SARAL/AltiKa track. J. Mar. Syst. 179, 55–71.

Calafat, F.M., Cipollini, P., Bouffard, J., Snaith, H., Féménias, P., 2017. Evaluation of new CryoSat-2 products over the ocean. Remote Sens. Environ. 191, 131–144.

Chelton, D.B., Ries, J.C., Haines, B.J., Fu, L.-L., Callahan, P.S., 2001. Chapter 1 Satellite Altimetry. In: Fu, L.-L., Cazenave, A., (Eds.). International Geophysics. Academic Press, 1-ii.

Dung, T.T., Kulinich, R.G., Van Sang, N., et al., 2019. Improving accuracy of altimeter-derived marine gravity anomalies for geological structure research in the vietnam south-central continental shelf and adjacent areas. Russian J. Pacific Geol. 13, 364–374.

ESA-ESTEC, 2007. CryoSat Mission and Data Description. European Space Agency ESTEC, Noordwijk, The Netherlands.

Fairhead, J.D., Green, C.M., Odegard, M.E., 2001. Satellite-derived gravity having an impact on marine exploration. Lead. Edge 20, 873–876.

Fenoglio-Marc, L., Dinardo, S., Scharroo, R., et al., 2015. The German Bight: A validation of CryoSat-2 altimeter data in SAR mode. Adv. Space Res. 55, 2641–2656.

Forsberg, R., Tscherning, C.C., 2008. An overview manual for the GRAVSOFT Geodetic Gravity Field Modelling Programs.

Fu, L.L., Christensen, E.J., Yamarone, C.A., et al., 1994. TOPEX/POSEIDON mission overview. J. Geophys. Res. Oceans 99, 24369–24381.

Gaina, C., Müller, R.D., Roest, W.R., Symonds, P., 1998. The opening of the tasman sea: a gravity anomaly animation. Earth Interact 2, 1–23.

Gao, J., Xue, H., Chai, F., Shi, M., 2013. Modeling the circulation in the Gulf of Tonkin, South China Sea. Ocean Dyn. 63, 979–993.

Hackney, R.I., Featherstone, W.E., 2003. Geodetic versus geophysical perspectives of the 'gravity anomaly'. Geophys. J. Int. 154, 35–43.

Haxby, W.F., Karner, G.D., LaBrecque, J.L., Weissel, J.K., 1983. Digital images of combined oceanic and continental data sets and their use in tectonic studies. Eos, Trans. Am. Geophys. Union 64, 995–1004.

Hofmann-Wellenhof, B., Moritz, H., 2006. Physical Geodesy.

Hwang, C., Hsu, H.-Y., Deng, X., 2004. Marine gravity anomaly from satellite altimetry: a comparison of methods over shallow waters. In: Hwang, C., Shum, C.K., Li, J. (Eds.), Satellite Altimetry for Geodesy, Geophysics and Oceanography. Springer, Berlin Heidelberg, Berlin, Heidelberg, pp. 59–66.

Hwang, C., Hsu, H.Y., Jang, R.J., 2002. Global mean sea surface and marine gravity anomaly from multi-satellite altimetry: applications of deflection-geoid and inverse Vening Meinesz formulae. J. Geod. 76, 407–418.

Hwang, C., Parsons, B., 1996. An optimal procedure for deriving marine gravity from multi-satellite altimetry. Geophys. J. Int. 125, 705–718.

ICGEM. Root mean square (rms) about mean of GPS / levelling minus gravity field model derived geoid heights [m]. GFZ.

ICGEM, 2019. Root mean square (rms) about mean of GPS / levelling minus gravity field model derived geoid heights [m]. http://icgem.gfz-potsdam.de/tom_gpslev. Helmholtz Center Potsdam.

Idžanović, M., Ophaug, V., Andersen, O.B., 2017. The coastal mean dynamic topography in Norway observed by CryoSat-2 and GOCE. Geophys. Res. Lett. 44, 5609–5617.

Liu, L., Jiang, X., Liu, S., et al., 2016. Calculating the marine gravity anomaly of the South China Sea based on the Inverse Stokes Formula. IOP Conference Series: Earth and Environmental Science 46, 012062.

Marks, K.M., 1996. Resolution of the Scripps/NOAA Marine Gravity Field from satellite altimetry. Geophys. Res. Lett. 23, 2069–2072.

Minh, N.N., Patrick, M., Florent, L., et al., 2014. Tidal characteristics of the gulf of Tonkin. Cont. Shelf Res. 91, 37–56.

Nguyên Tính, T. Đi u tra đ c đi m đ a ch t, đ a đ ng lực, đ a ch t khoáng sản, đ a ch t môi trường và dự báo tai bi n đ a ch t vùng bi n Vi t Nam từ đ sâu 30m nước đ n 100m nước, tỷ l 1:500.000. Ministry of Natural Resources & Environment of Vietnam, 2012.

Noréus, J.P., Nyborg, M.R., Hayling, K.L., 1997. The gravity anomaly field in the Gulf of Bothnia spatially characterized from satellite altimetry and in situ measurements. J. Appl. Geophys. 37, 67–84.

Rio, M.-H., Hernandez, F., 2004. A mean dynamic topography computed over the world ocean from altimetry, in situ measurements, and a geoid model. J. Geophys. Res. Oceans 109.

Ruiz Etcheverry, L.A., Saraceno, M., Piola, A.R., Valladeau, G., Möller, O.O., 2015. A comparison of the annual cycle of sea level in coastal areas from gridded satellite altimetry and tide gauges. Cont. Shelf Res. 92, 87–97.

Sandwell, D.T., 1992. Antarctic marine gravity field from high-density satellite altimetry. Geophys. J. Int. 109, 437–448.

Sandwell, D.T., Harper, H., Tozer, B., Smith, W.H.F., 2019. Gravity field recovery from geodetic altimeter missions. Adv. Space Res.

Sandwell, D.T., McAdoo, D.C., 1988. Marine gravity of the southern ocean and Antarctic margin from Geosat. J. Geophys. Res. Solid Earth 93, 10389–10396.

Sandwell, D.T., Müller, R.D., Smith, W.H., Garcia, E., Francis, R., 2014. New global marine gravity model from CryoSat-2 and Jason-1 reveals buried tectonic structure. Science 346, 65–67.

Sandwell, D.T., Smith, W.H., 2009a. Global marine gravity from retracked Geosat and ERS-1 altimetry: Ridge segmentation versus spreading rate. J. Geophys. Res.: Solid Earth, 114.

Sandwell, D.T., Smith, W.H.F., 1997. Marine gravity anomaly from Geosat and ERS 1 satellite altimetry. J. Geophys. Res. Solid Earth 102, 10039–10054.

Sandwell, D.T., Smith, W.H.F., 2009b. Global marine gravity from retracked Geosat and ERS-1 altimetry: Ridge segmentation versus spreading rate. J. Geophys. Res.: Solid Earth, 114.

Sansò, F., Sideris, M., 2013. Geoid Determination: Theory and Methods.

Shen, X., Zhang, J., Zhang, X., Meng, J., Ke, C., 2017. Sea ice classification using cryosat-2 altimeter data by optimal classifier-feature assembly. IEEE Geosci. Remote Sens. Lett. 14, 1948–1952.

Subrahmanyam, C., Thakur, N.K., Gangadhara Rao, T., Khanna, R., Ramana, M.V., Subrahmanyam, V., 1999. Tectonics of the Bay of Bengal: new insights from satellite-gravity and ship-borne geophysical data. Earth Planet. Sci. Lett. 171, 237–251.

Thao, N.H., 2005. Maritime Delimitation and fishery cooperation in the Tonkin Gulf. Ocean Development & International Law 36, 25–44.

Tournadre, J., Bouhier, N., Boy, F., Dinardo, S., 2018. Detection of iceberg using Delay Doppler and interferometric Cryosat-2 altimeter data. Remote Sens. Environ. 212, 134–147.

Trung, N.N., Hong, P.T., Van Nam, B., Huong, N.T.T., Lap, T.T., 2018. Moho depth of the northern Vietnam and Gulf of Tonkin from 3D inverse interpretation of gravity anomaly data. J. Geophys. Eng. 15, 1651–1662.

Tscherning, C.C., Rapp, R., 1974. Closed covariance expressions for gravity anomalies, geoid undulations, and deflections of the vertical implied by anomaly degree variance models.

Verron, J., Bonnefond, P., Aouf, L., et al., 2018. The benefits of the Ka-band as evidenced from the SARAL/AltiKa altimetric mission: Scientific applications. Remote Sens. 10, 163.

Verron, J., Sengenes, P., Lambin, J., et al., 2015. The SARAL/AltiKa Altimetry satellite mission. Mar. Geod. 38, 2–21.

Vu, T.S., Nguyen, B., Dao, M.T., Duong, V.H., Le, V.H., Le, A.T., 2009. Some results of investigations on geology and minerals coastal shallow waters of Vietnam Center for Marine Geology and Minerals, Hanoi, Vietnam.

Zhang, C., Blais, J.A.R., 1995. Comparison of methods for marine gravity determination from satellite altimetry data in the Labrador Sea. Bull. géodésique 69, 173.

Zhang, S., Sandwell, D., Jin, T., Li, D., 2017. Inversion of marine gravity anomalies over southeastern China seas from multi-satellite altimeter vertical deflections. J. Appl. Geophys. 137, 128–137.

Zhang, Y., Zhang, J., Ji, Y., Zhang, H., 2003. Calculation of geoid undulations and gravity anomalies in the South China Sea by using the TOPEX/Poseidon and Geosat altimeter data. Proc. SPIE - The Int. Soc. Opt. Eng. 4892.